Principles and Practice of Clinical Electrophysiology of Vision

Editors

JOHN R. HECKENLIVELY, M.D.
Professor of Ophthalmology
Jules Stein Eye Institute
Los Angeles, California

GEOFFREY B. ARDEN, M.D., PH.D.
Professor of Ophthalmology and Neurophysiology
Institute of Ophthalmology
Moorfields Eye Hospital
London, England

Associate Editors

EMIKO ADACHI-USAMI, M.D.
Professor of Ophthalmology
Chiba University School of Medicine
Chiba, Japan

G.F.A. HARDING, PH.D.
Professor of Neurosciences
Department of Vision Sciences
Aston University
Birmingham, England

SVEN ERIK NILSSON, M.D., PH.D.
Professor of Ophthalmology
University of Linköping
Linköping, Sweden

RICHARD G. WELEBER, M.D.
Professor of Ophthalmology
University of Oregon Health Science Center
Portland, Oregon

Mosby Year Book

St Louis Baltimore Boston Chicago London Philadelphia Sydney Toronto

Mosby
Year Book

Dedicated to Publishing Excellence

Sponsoring Editor: David K. Marshall
Assistant Director, Manuscript Services: Frances M. Perveiler
Production Project Coordinator: Karen E. Halm
Proofroom Manager: Barbara Kelly

A Year Book Medical Publishers imprint of Mosby-Year Book, Inc.

Mosby-Year Book, Inc.
11830 Westline Industrial Drive
St. Louis, MO 63146

1 2 3 4 5 6 7 8 9 0 CL CL MV 95 94 93 92 91

Library of Congress Cataloging-in-Publication Data
Principles and practice of visual electrophysiology / [edited by]
John R. Heckenlively, Geoffrey B. Arden.
p. cm.
Includes bibliographical references.
Includes index.
ISBN 0-8151-4290-0
1. Electroretinography. 2. Electrooculography. 3. Visual evoked response. I. Heckenlively, John R. II. Arden, Geoffrey B. (Geoffrey Bernard)
[DNLM: 1. Electrooculography. 2. Electrophysiology. 3. Electroretinography. 4. Evoked Potentials, Visual. 5. Vision Disorders—physiopathology. WW 270 P957]
RE79.E4P75 1991 91-13378
617.7 1547—dc20 CIP
DNLM/DLC
for Library of Congress

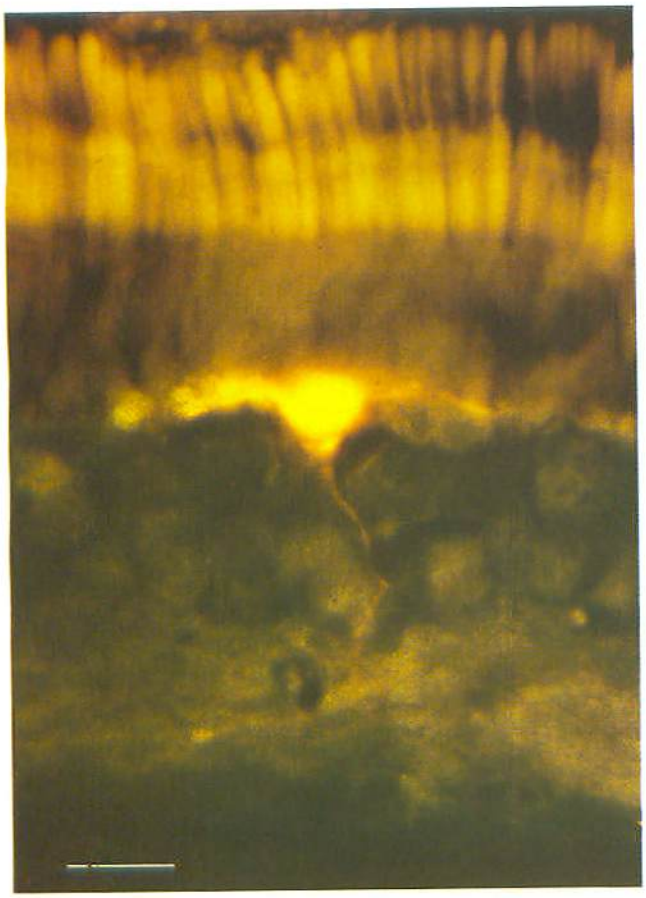

PLATE 1.—A radial section through the retina of the dogfish as viewed in a fluorescence microscope. In the center of the field is a rod on bipolar cell that had been injected with a nontoxic fluorescent dye while in situ in the living retina and that responded to light as in Figure 7–9,A. The rod layer is in the *upper part* of the figure, with the outer segments being strongly autofluorescent. A fine axon of the bipolar cell can be traced deep into the inner plexiform layer and terminates as a bulbous process (calibration bar, 25 μm). (From Ashmore JF, Falk G: *J Physiol* 1980; 300:115–150. Used by permission.) **(See also Fig 7–10.)**

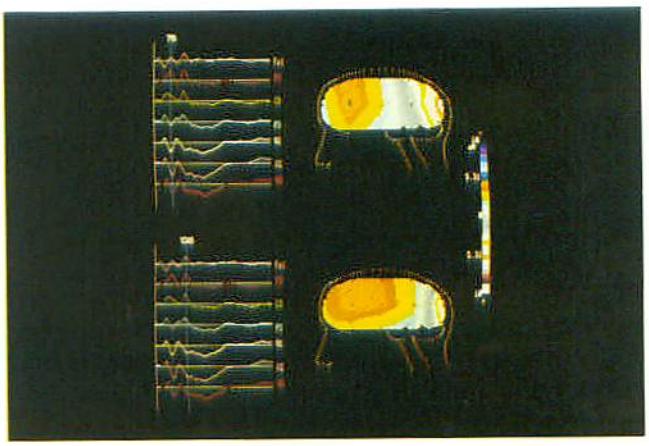

PLATE 2.—Distribution of both the P1 and P2 components of the flash VEP. The P1 component seen in the *upper* block of traces and the upper anteroposterior brain map spreads more anteriorly than does the P2 component seen in the *lower* traces and lower brain map. It should be noted that the positivity of the P1 and P2 components (as indicated in the scale on the *right*) are accompanied by frontal negative potentials occurring at the same time. These recordings were made by using a balanced noncephalic reference. **(See also Fig 18–2.)**

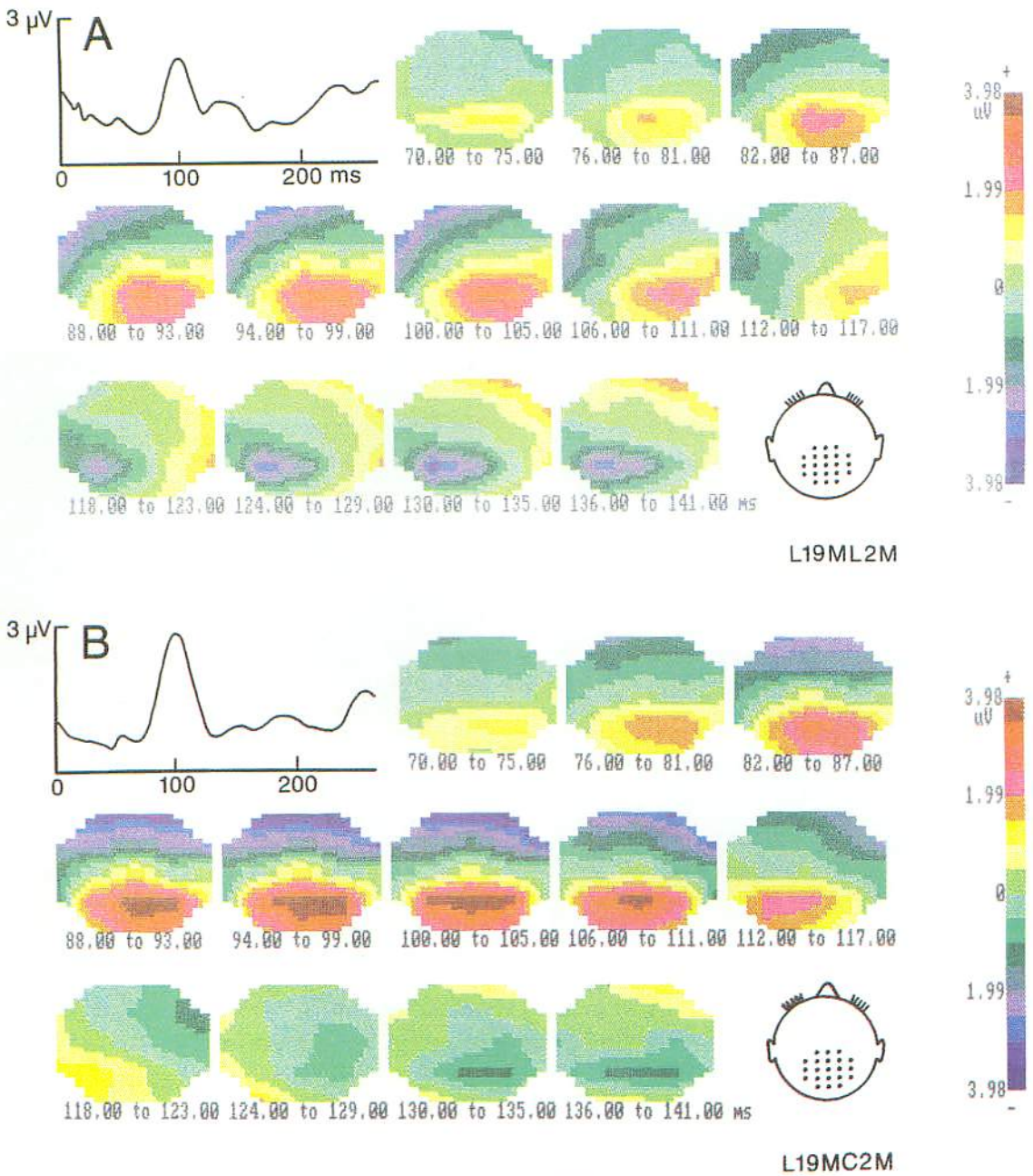

PLATE 3.—Potential map series between 70 and 141 ms and GFP as a function of time evoked by a contrast-reversing vertical grating stimulus of 2.5 cd presented monocularly as a 17.1-by-13.4-degree arc test field in the center **(B)** or to the left **(A)** or right hemiretinas **(C).** In all map series an occipital positive component develops around 100 ms and shows some lateralization with lateral visual stimuli. Values are means of average reference data; 21 channels were recorded by using a *BioLogic Brain Atlas II* with the most anterior electrode row at 40% of the nasion-inion distance above the inion and the most posterior electrode row at the inion. Potential levels are color coded between +3.98 and −3.98 μV as indicated in scale on the *right.* **(See also Fig 33–6.)**

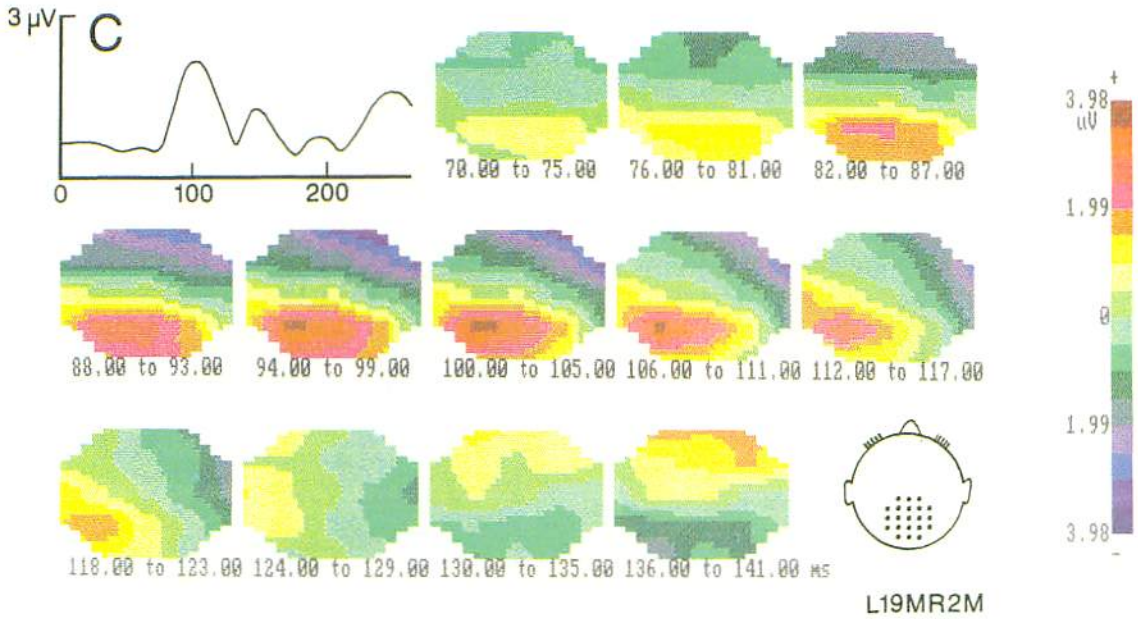

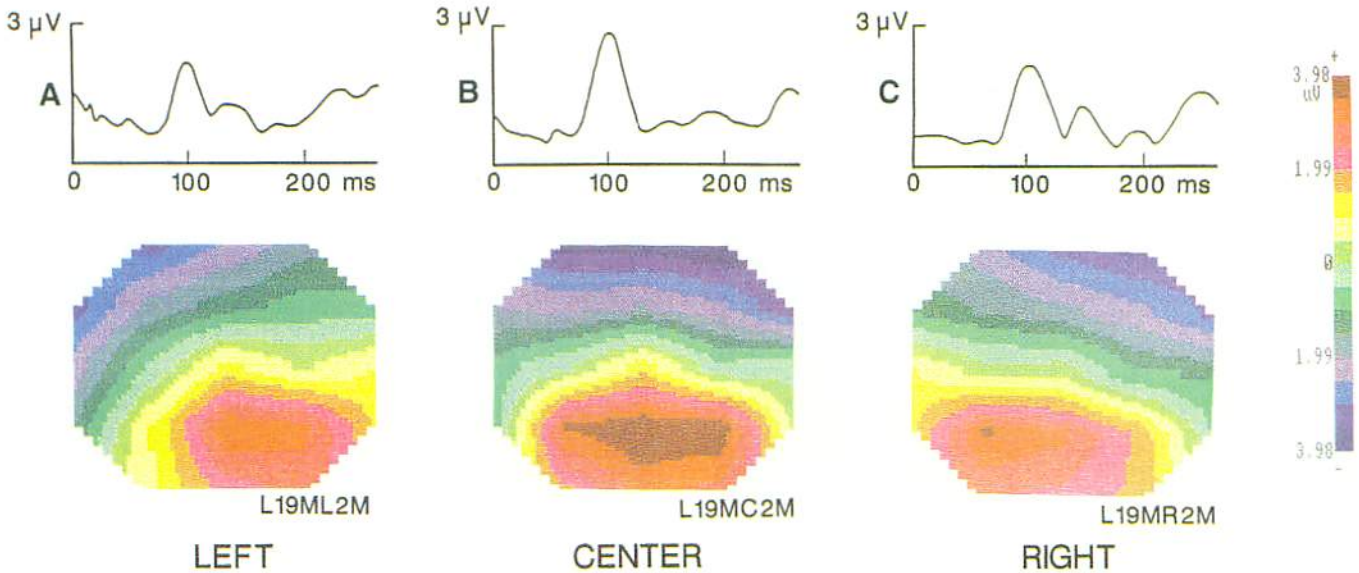

PLATE 4.—GFP functions and EP maps at component latency of the data presented in Figure 33–6. With central stimuli **(B)** the occipital positivity is located concentrically in the midline, while with left **(A)** or right **(C)** hemiretinal stimuli the maximum is located over the hemisphere contralateral to the hemiretina stimulated, and there occur steep potential gradients over the ipsilateral hemisphere. Note the larger field strength with central than with lateral stimuli. Component latencies are similar in all conditions. Potential levels are color coded between +3.98 and −3.98 μV as indicated in scale on the *right*. **(See also Fig 33–7.)**

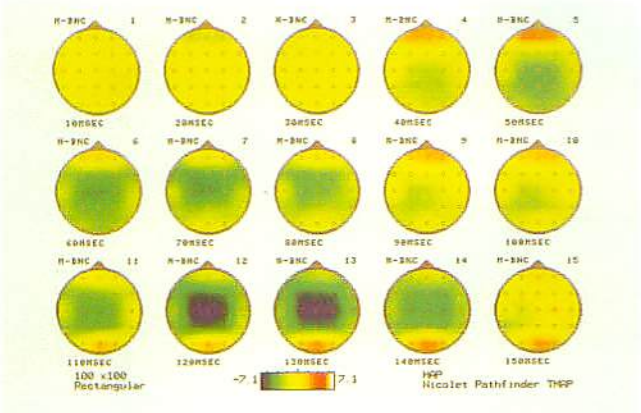

PLATE 5.—Distribution of activity across the scalp in 10-ms steps from flash stimulation. The brain maps indicate electrode positions according to the 10:20 system, and each electrode is referred to a balanced noncephalic reference. The diagram shows the group average responses from normal middle-aged adults. It can be seen that between 50 and 80 ms there is a clear negativity in the frontal regions that is unaccompanied by any change in the occipital derivations. A little later, maximally around 120 and 130 ms, there is a clear positive P2 component developed in the occipital derivations that coexists with a marked negativity seen in frontal derivations. The fact that the earlier N75 component seen in the frontal regions does not coexist with the posterior component suggests that this may well be independent of activity in the occipital region. **(See also Fig 51–4.)**

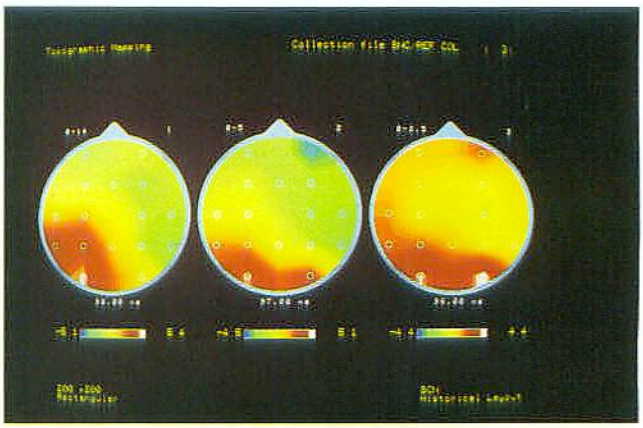

PLATE 6.—Topographical distribution of the P100 component of the VEP in response to left half-field stimulation with differing check sizes with a 0- to 14-degree-radius checkerboard consisting of elements subtending 56 minutes of visual angle. It can be seen that the response is ipsilateral to the half-field stimulated as indicated as a marked positive component around 90 ms that is maximal over the left occiput (*white* and *red*). As the field size is reduced to a 0- to 5-degree radius, the response, although remaining ipsilateral to the field stimulated, becomes more bilateral. With a 0- to 2.5-degree-radius field the response becomes crosslateral and is seen as a higher-amplitude response over the right occiput; this is indicated in *white* on the brain map. **(See also Fig 55–1.)**

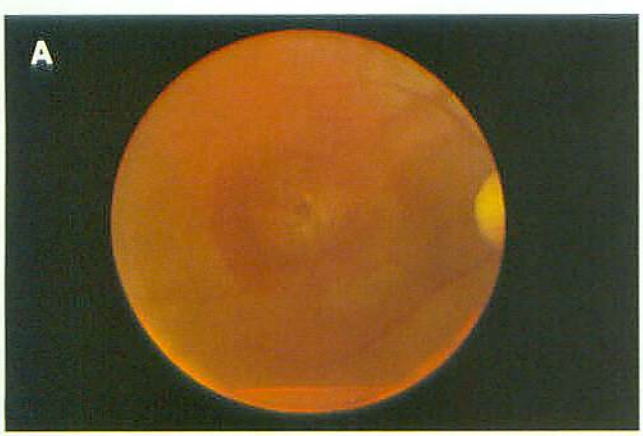

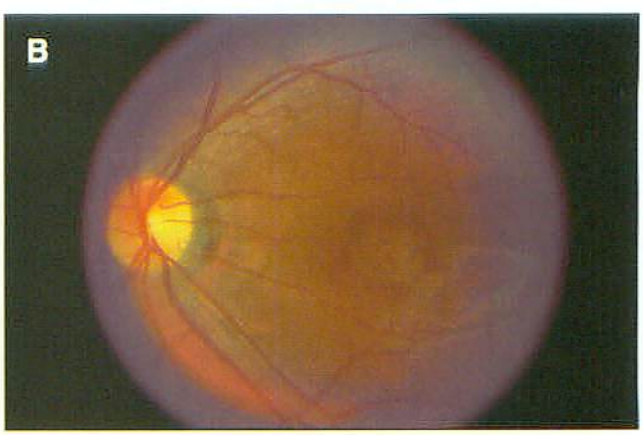

PLATE 7.—**A** and **B,** bull's-eye macular lesion in an aunt and nephew, both in their early twenties, with autosomal dominant cone dystrophy. These patients' conditions could be mistaken for examples of Stargardt's disease or fundus flavimaculatus; the ERG will differentiate these retinal pigment epithelial diseases from cone degeneration. **(See also Fig 67–2.)**

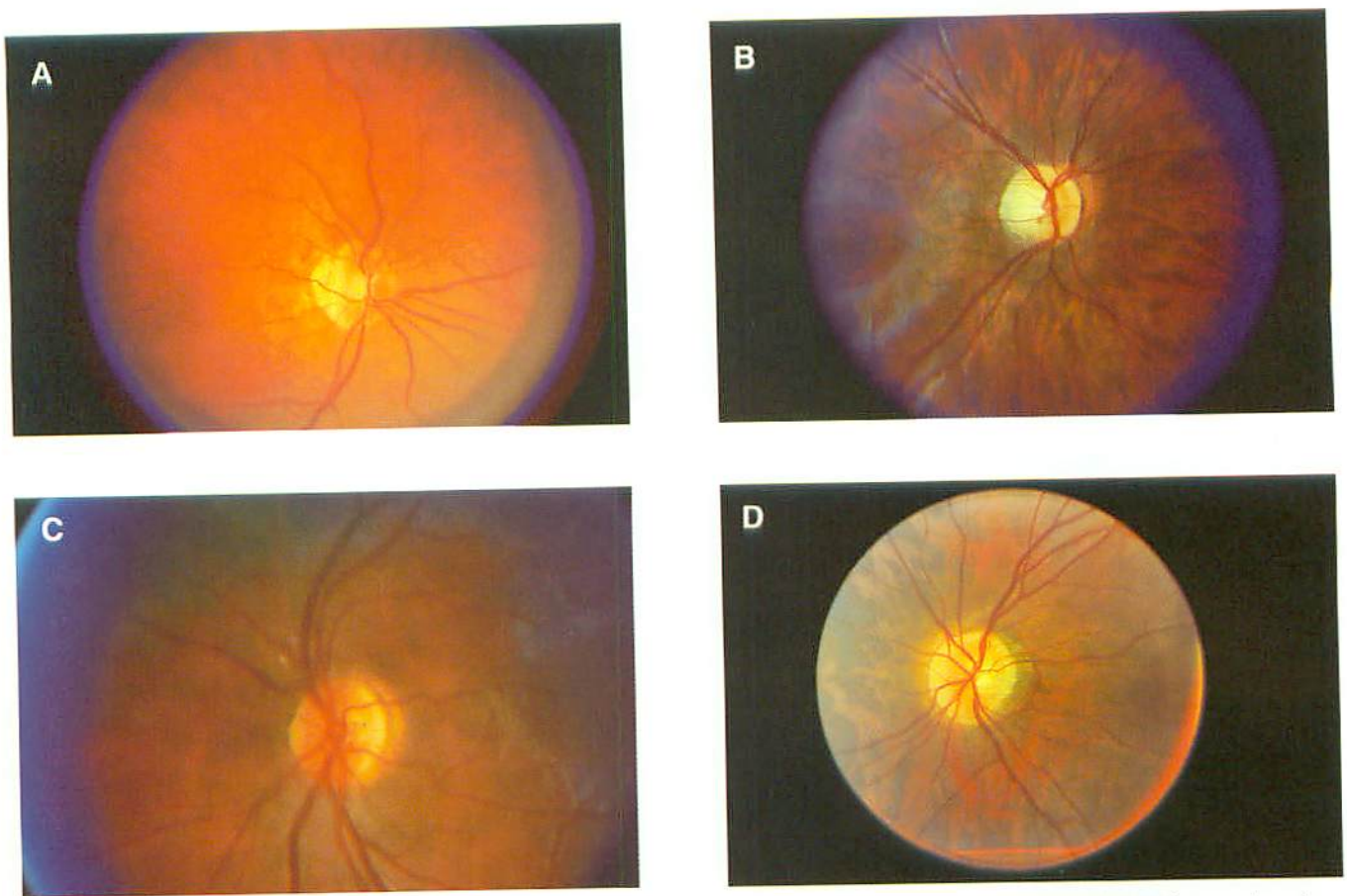

PLATE 9.—Temporal optic atrophy in cone degeneration. **A,** a 51-year-old man with blue cone monochromatism and a missing temporal disc. **B,** a 9-year-old boy with rod monochromatism and temporal pallor. **C,** a 12-year-old boy with sporadic cone degeneration and a temporal wedge of pallor. **D,** a 28-year-old man with acquired cone degeneration and a granular glistening edge of the disc atrophy. This latter finding is occasionally seen in RP and, while similar to disc drusen, is localized temporally. **(See also Fig 67–4.)**

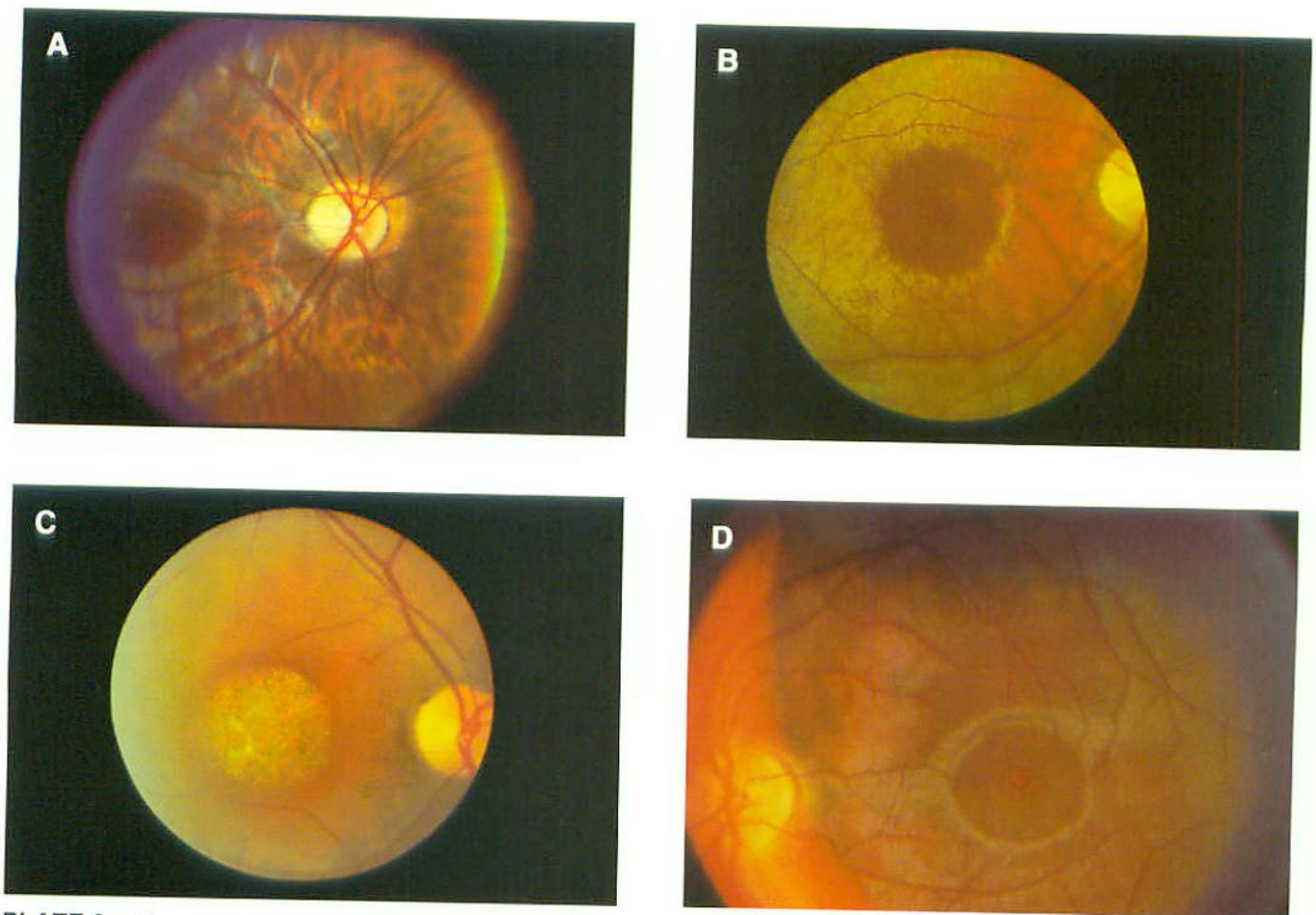

PLATE 8.—Concentric atrophy of the fovea centralis is often seen in a number of types of cone dystrophy or degeneration. **A,** a 9-year-old boy with autosomal recessive rod monochromatism in which retinal surface reflections are lost in an area of round foveal atrophy. **B,** a 54-year-old man with X-linked cone dystrophy and a tapetal-like sheen highlighting and surrounding the foveal atrophy. **C,** a 48-year-old woman with autosomal dominant cone dystrophy with macular atrophy. Many of these patients show hyperpigmentation of the retinal pigment epithelium at the edge of the macular atrophy. **D,** a 12-year-old boy with acquired sporadic cone degeneration with symmetrical foveal atrophy; retinal vessels curve into the depression caused by the atrophy as seen in Figure 67–3, B and D. **(See also Fig 67–3.)**

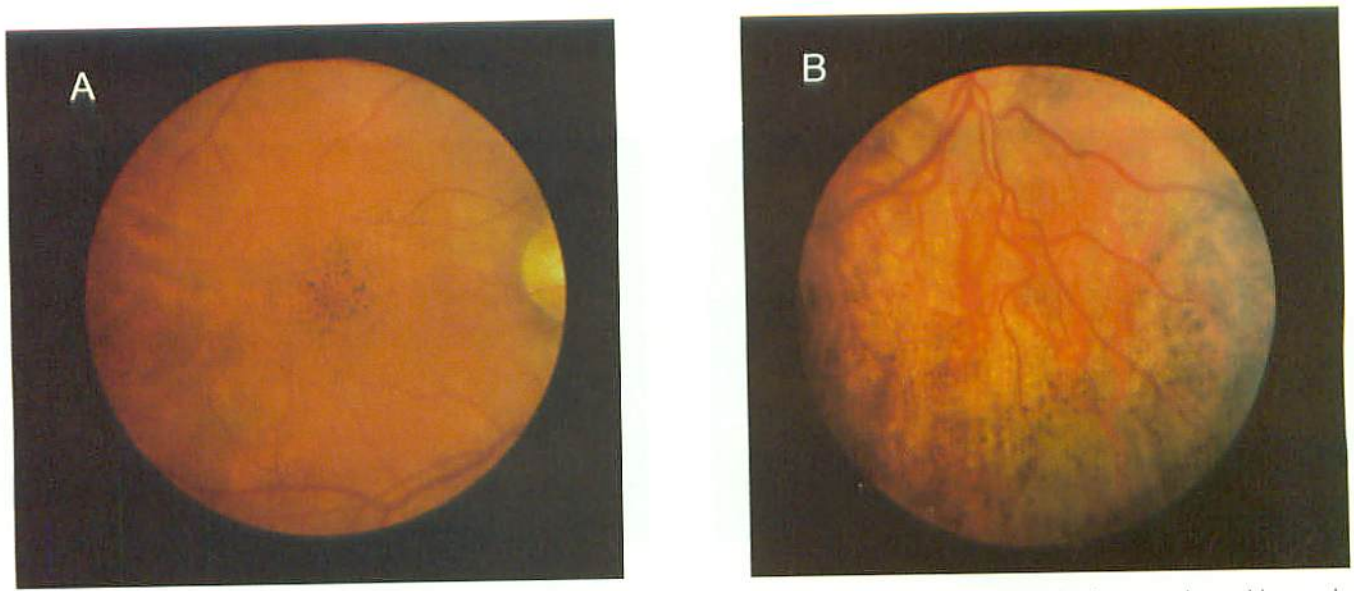

PLATE 10.—Examples of early thioridazine retinopathy. Coarse granular pigmentation is present in the macula and beyond. **(See also Fig 78–2.)**

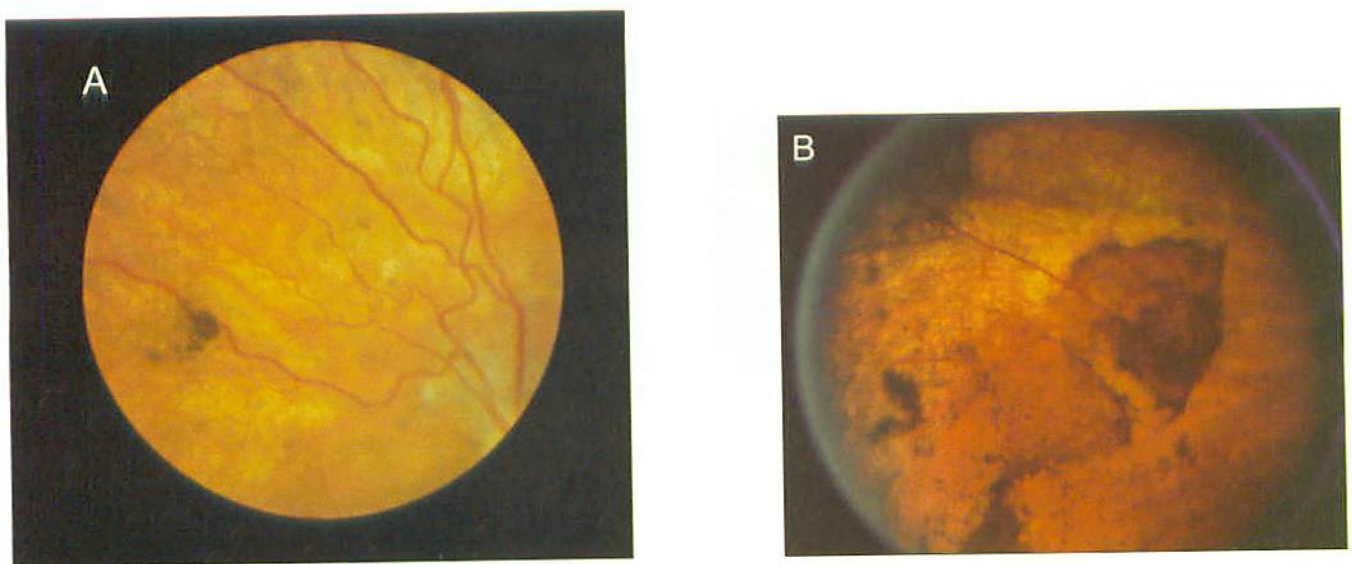

PLATE 11.—Examples of late thioridazine retinopathy. The appearance has changed to a nummular pattern of atrophic and hyperpigmented patches. **(See also Fig 78–3.)**

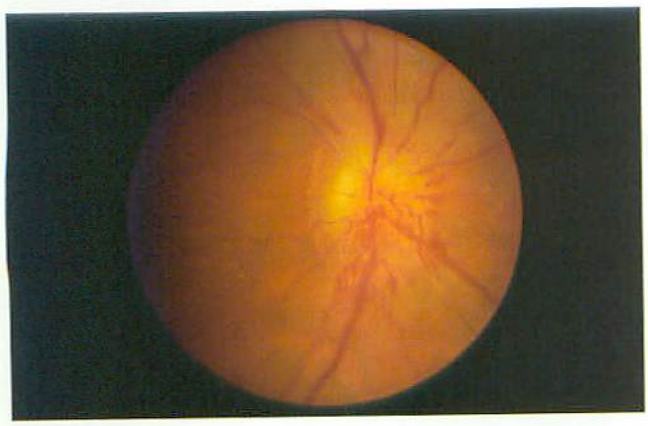

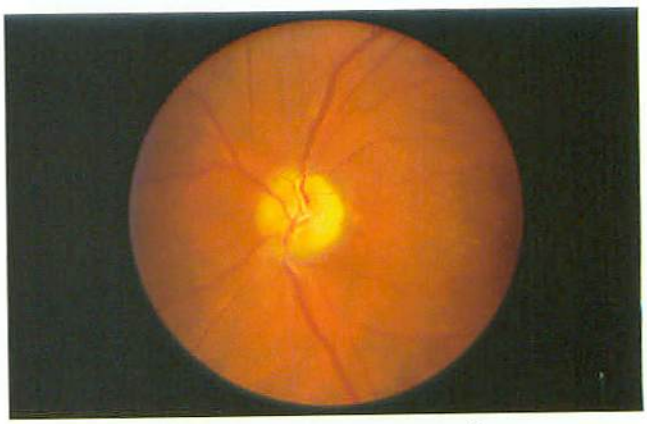

PLATE 12.—Fundus photograph in patient with pseudo-Foster-Kennedy syndrome due to acute ischemic optic neuropathy; right eye *(left)* shows marked disc swelling, while left eye *(right)* has old ischemic changes with an atrophic disc. The PVEPs from both eyes are of subnormal amplitude with no definite latency change. **(See also Fig 82–3.)**

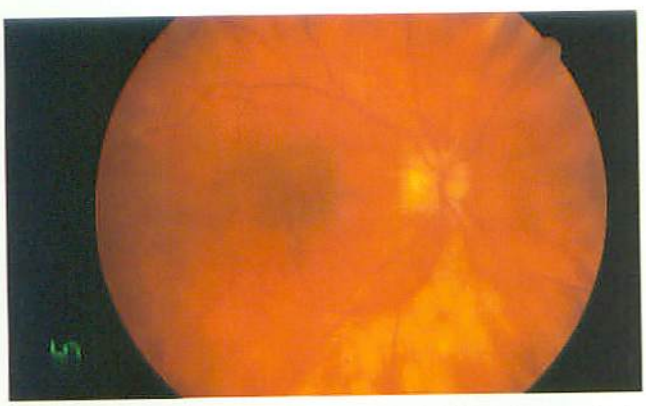

PLATE 13.—Fundus appearance in birdshot choreoretinitis. Pale fundus lesions are neither raised nor depressed relative to the surrounding retina. (Courtesy of L. Yannuzzi, M.D.) **(See also Fig 83–1.)**

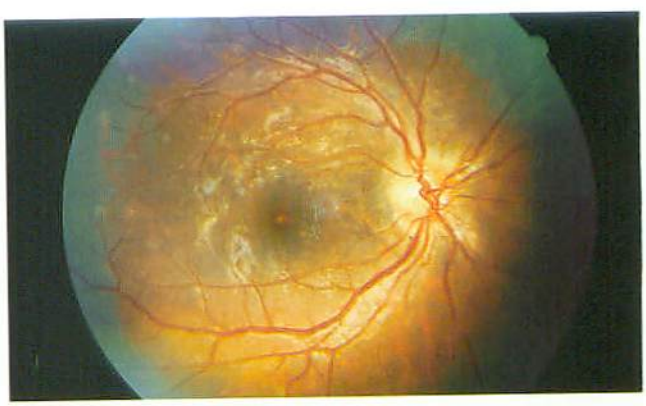

PLATE 14.—Fundus appearance in MEWDS. (Courtesy of L. Jampol, M.D., and G. Fishman, M.D.) **(See also Fig 83–2.)**

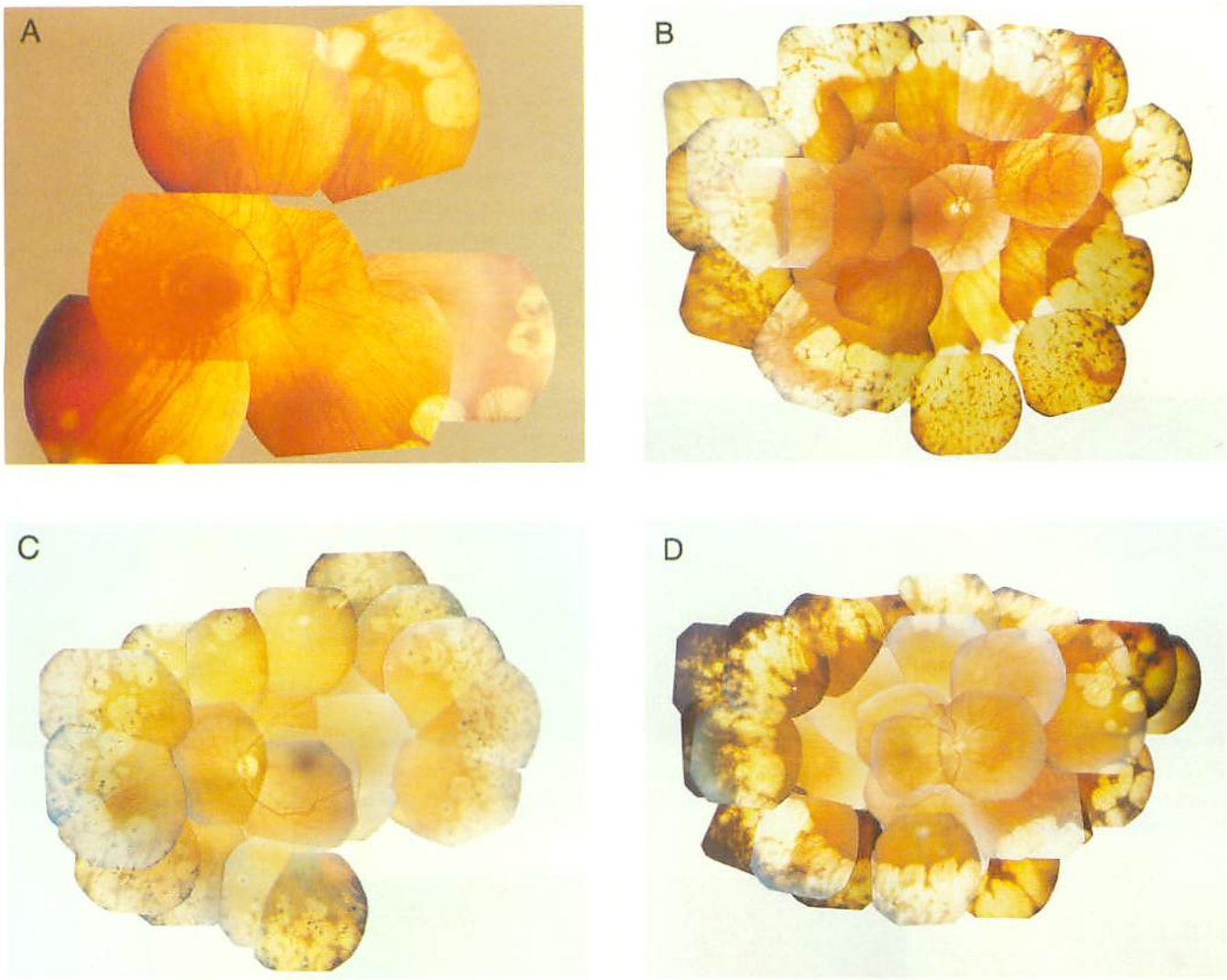

PLATE 15.—Fundus appearance **A,** right eye, 15-year-old girl with early pyridoxine-nonresponsive gyrate atrophy (same patient as in Fig 12–1, Weleber and Kennaway[46]). **B,** a 28-year-old with pyridoxine-responsive gyrate atrophy (Patient 1). **C,** a 37-year-old woman with pyridoxine-responsive gyrate atrophy (Patient 3). **(D)** a 40-year-old man with pyridoxine-nonresponsive gyrate atrophy (Patient 4). (From Weleber RG, Kennaway NG: Gyrate atrophy of the choroid and retina, in Heckenlively JR (ed): *Retinitis Pigmentosa.* Philadelphia, JB Lippincott, 1988, pp 198–220. Used by permission.) **(See also Fig 85–4.)**

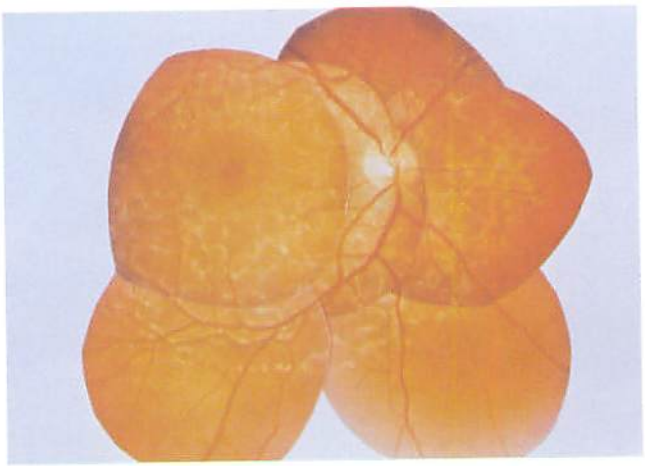

PLATE 16.—There are diffuse flecks in the posterior pole and beyond the vascular arcades. On scanning electron microscopy, the flecks are aggregations of swollen retinal pigment epithelial cells (see Eagle, 1981). The vision was 20/20, and the macula appeared unaffected. **(See also Fig 88–3.)**

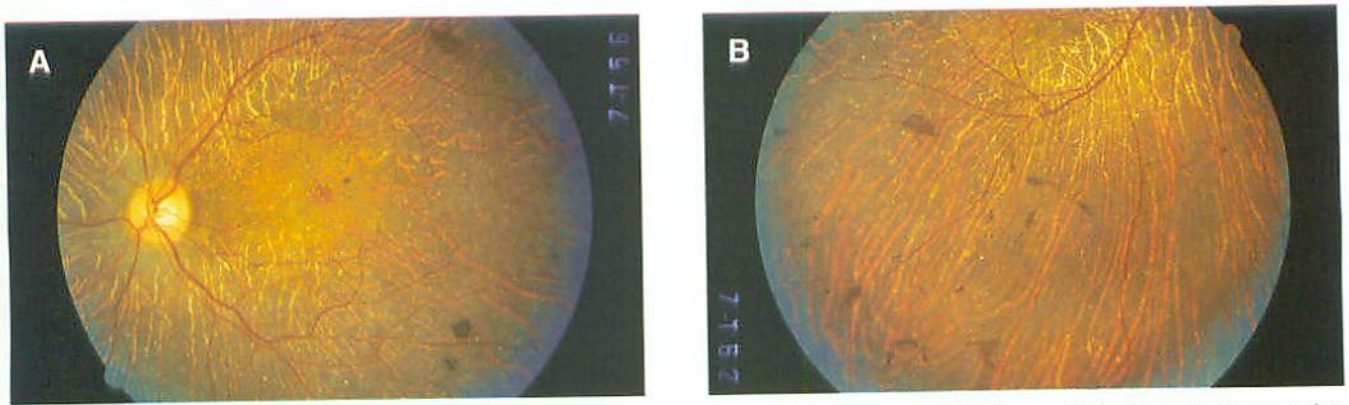

PLATE 17.—Patient at 45 years of age (**A** and **B**). Note the further loss of pigment epithelium and choriocapillaris over the 9-year interval. (From Wilson DJ, Weleber RG, Klein ML, Welch RB, Green WR: *Arch Ophthalmol* 1989; 107:213–221. Used by permission.) **(See also Fig 90–2.)**

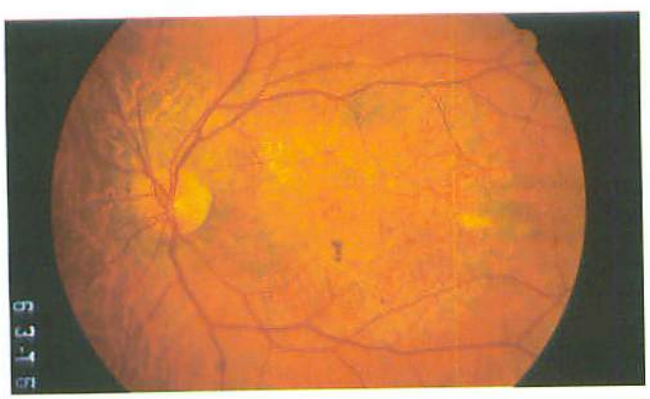

PLATE 18.—Fundus appearance of the left eye of a 61-year-old man with the regional form of Bietti's crystalline dystrophy (patient 3 in Wilson et al.[24]). The visual fields had not changed over those determined 9 years previously, but the visual acuity had decreased from 20/30 J1 to 20/40 J2. **(See also Fig 90–6.)**

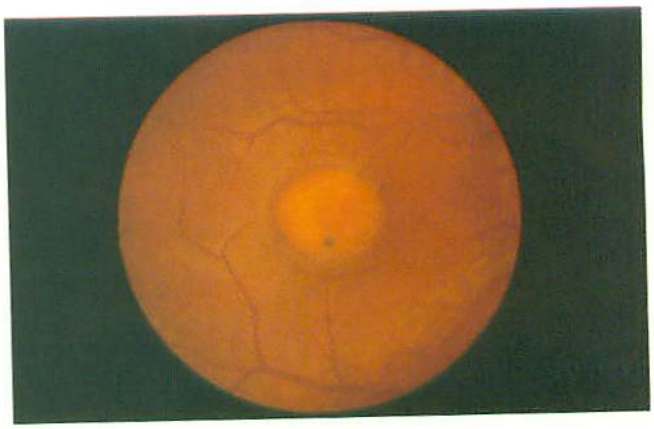

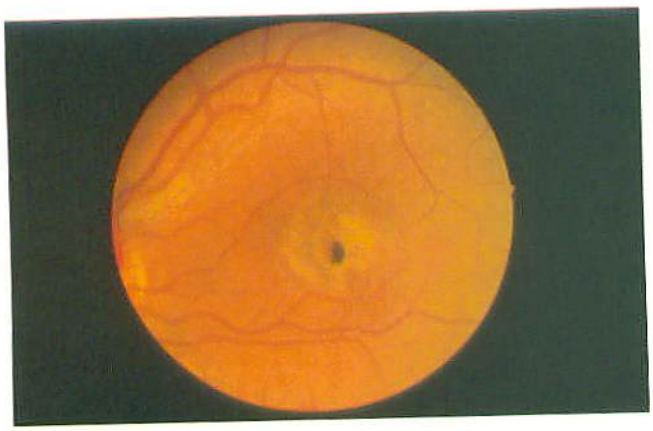

PLATE 19.—Fundus appearance of Best's disease. The female patient was born in 1964, and the fundus was photographed in 1977, 1983, and 1989. The EOG light peak/dark trough (LP/DT) ratio was 1.1 OU and did not change over the years. The visual acuity was 6/9 OD, 6/7.5 OS in 1977 and 6/7.5 OD, 6/6 OS in 1989. The size of the vitelliform lesion increased over a period of 6 years, the "cyst" was then absorbed, and a pigmented scar formed. The visual acuity, reflecting an unaffected neuroretina, did not change. (Courtesy of G. Frank Judisch, M.D.) **(See also Fig 91–1.)**

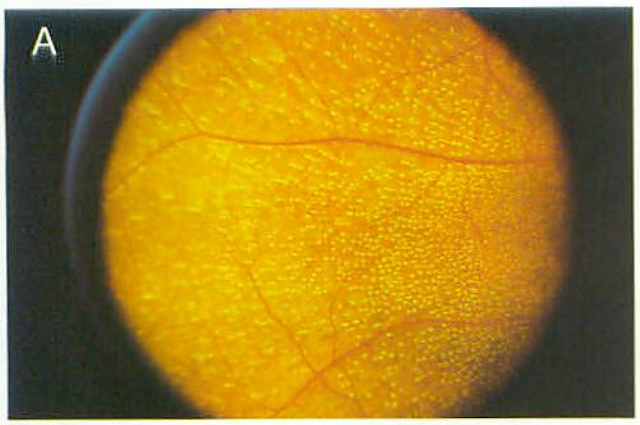

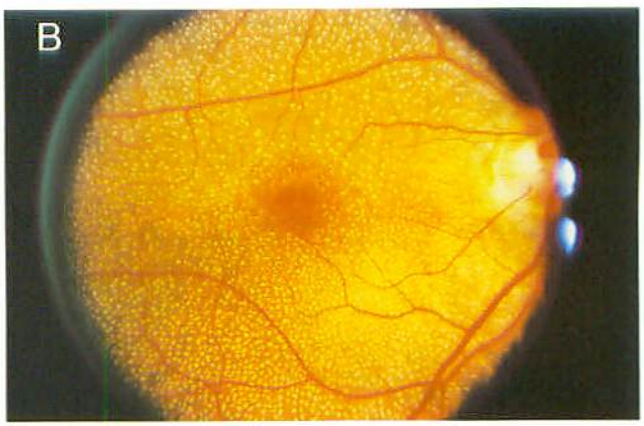

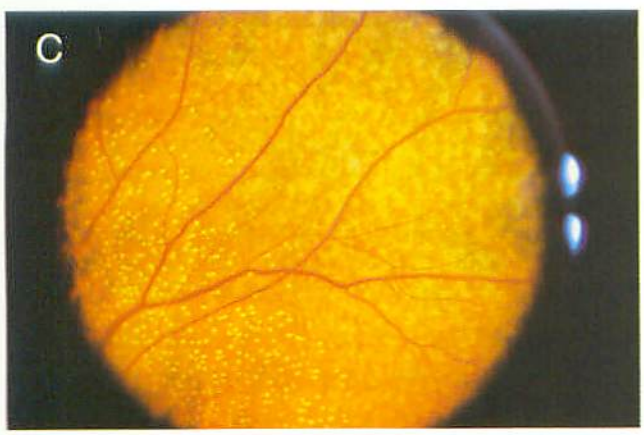

PLATE 20.—Fundus albipunctatus in a 38-year-old man. **A–C,** fundus photographs showing punctate dots centrally and radiating dots that become more flecklike peripherally. **(See also Fig 99–1.)**

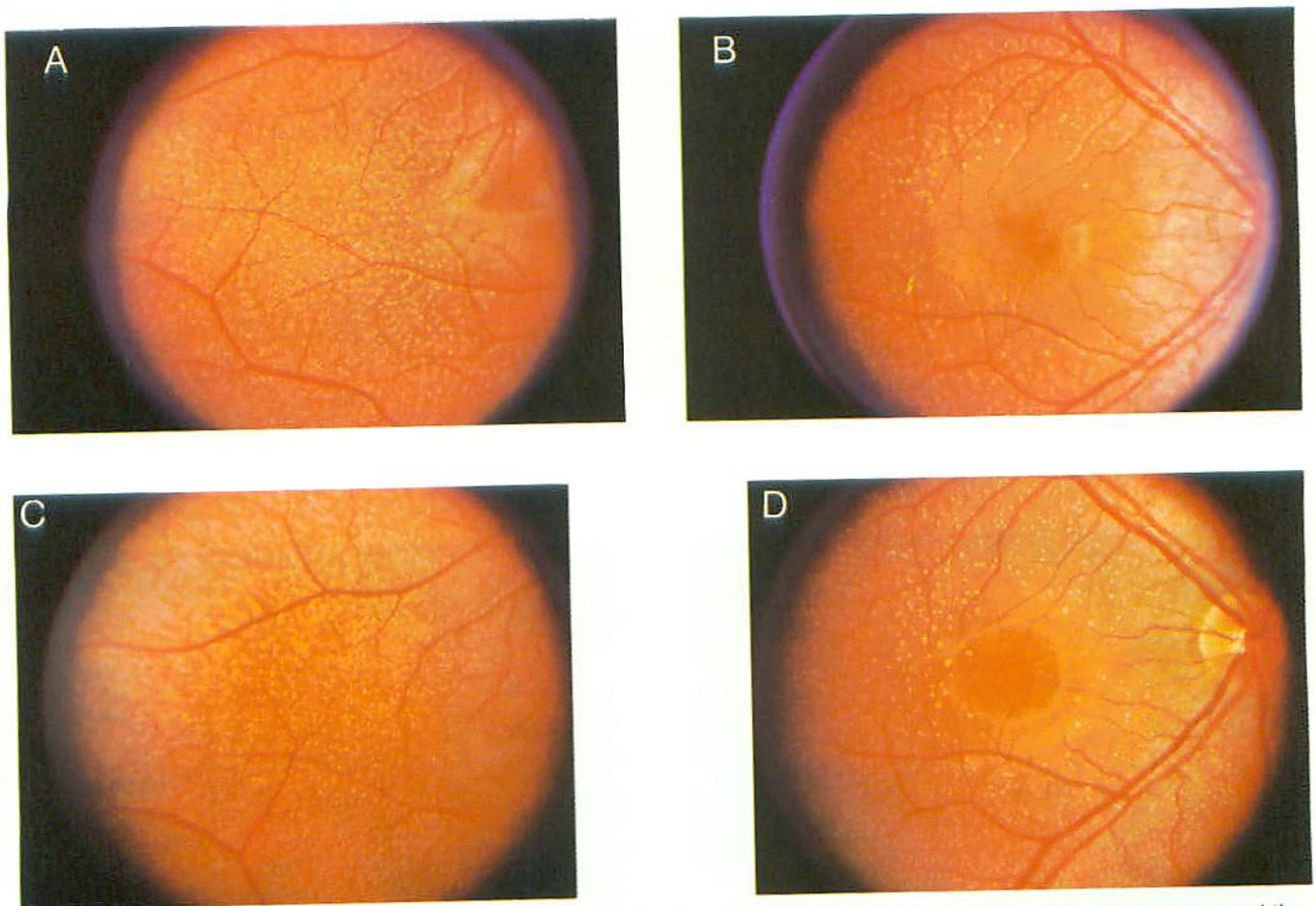

PLATE 21.—Fundus albipunctatus, age 8 (**A** and **B**) and age 21 years (**C** and **D**). Note the increase in macular dots and the conversion of many peripheral flecks to dots. **(See also Fig 99–2.)**

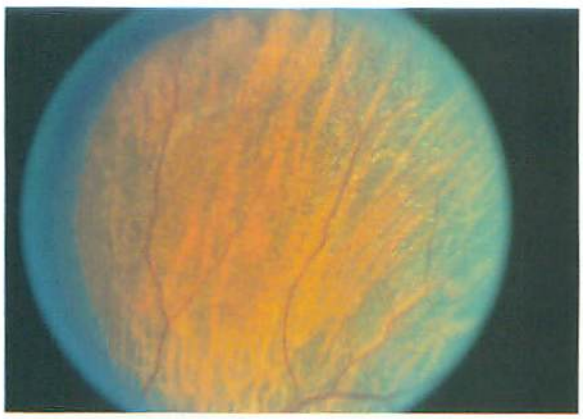

PLATE 22.—Fundus photograph of a 53-year-old woman with documented vitamin A deficiency from complications secondary to bowel resection in Crohn's disease. Her barely recordable ERG and night vision became normal after parenteral vitamin A and E therapy. (Courtesy of John Heckenlively, M.D.) **(See also Fig 100–1.)**

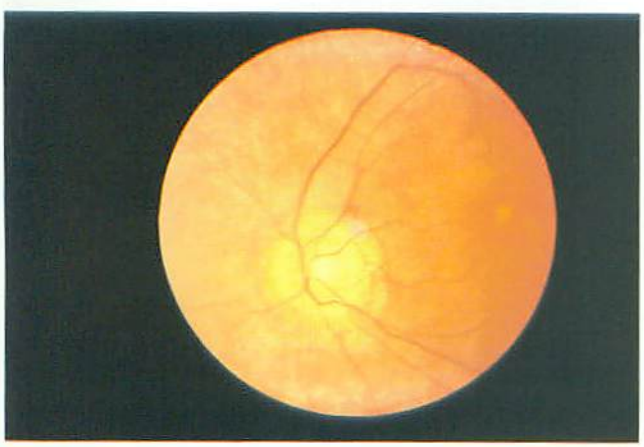

PLATE 23.—Fundus photograph of a 43-year-old XLRP heterozygote with "waxy pallor" of the optic disc and constricted retinal arterioles. **(See also Fig 101–1.)**

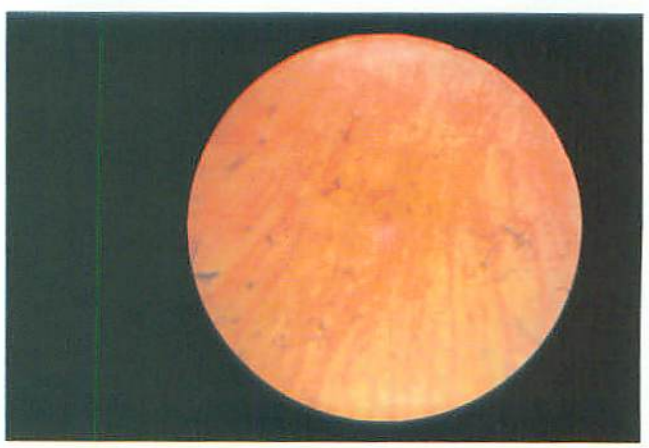

PLATE 24.—The peripheral retina of the XLRP carrier in Figure 102–1 with intraretinal "bone spicule" pigmentation. **(See also Fig 101–2.)**

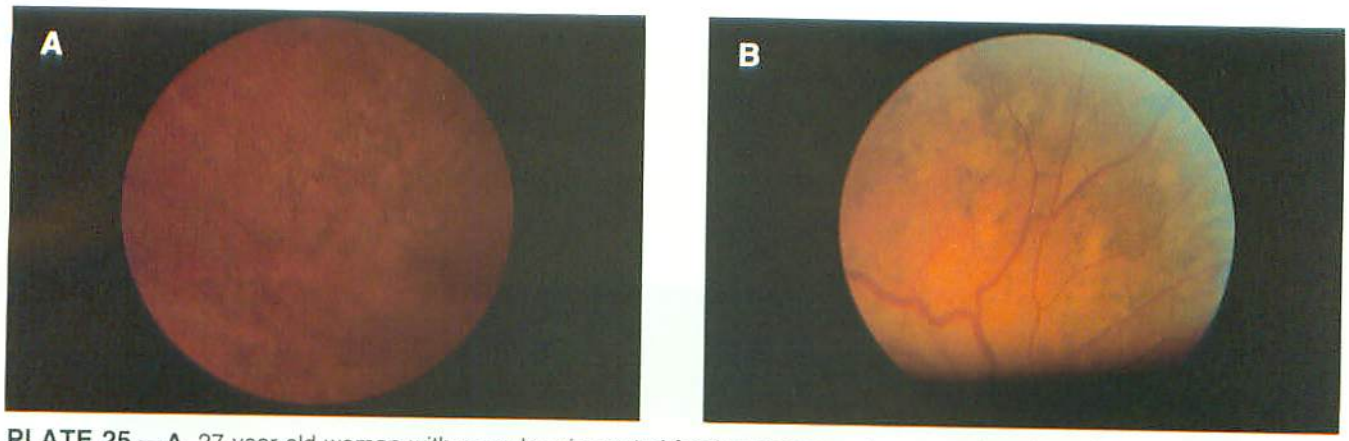

PLATE 25.—**A,** 27-year-old woman with granular pigmented fundus changes who was referred to rule out retinitis pigmentosa; she tested normally, but her brother was found to have choroideremia. **B,** 54-year-old woman who has two sons with choroideremia with granular atrophic patches in the equatorial regions. (Courtesy of John Heckenlively, M.D.) **(See also Fig 102–1.)**

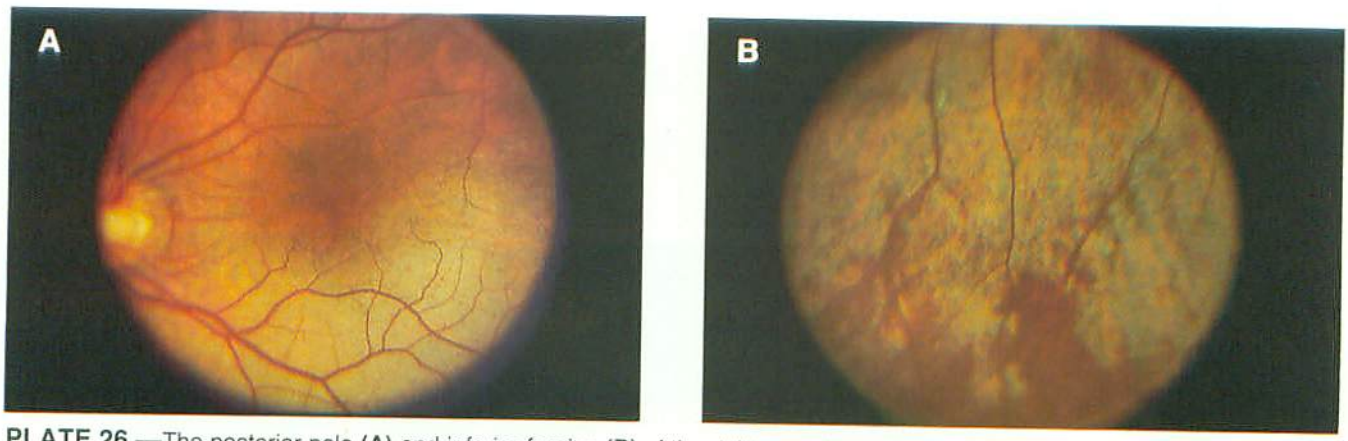

PLATE 26.—The posterior pole **(A)** and inferior fundus **(B)** of the right eye of a 13-year-old boy with X-linked cone dystrophy show a yellow tapetal-like reflex. (From Heckenlively JR, Weleber RG: *Arch Ophthalmol* 1986; 104:1322–1328. Used by permission.) **(See also Fig 105–1.)**

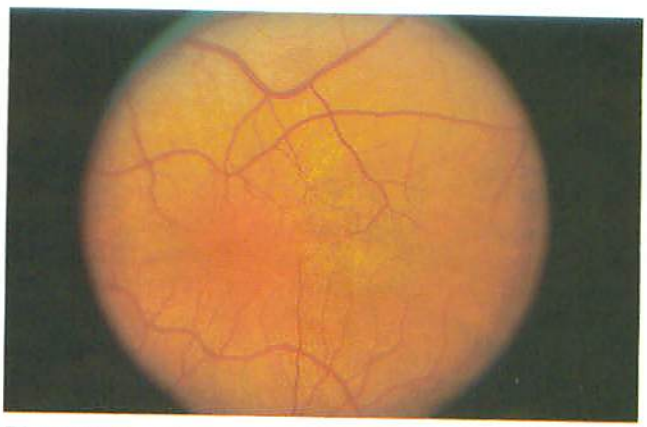

PLATE 27.—The macular region of the left eye of the 40-year-old mother of the patient shown in Figure 106–1 shows a faint tapetal-like reflex in the macular region. (From Heckenlively JR, Weleber RG: *Arch Ophthalmol* 1986; 104:1322–1328. Used by permission.) **(See also Fig 105–2.)**

PLATE 28.—Variable genotype and phenotype in a representative sample of albinos including autosomal recessive oculocutaneous tyrosinase negative albinism *(left column)*, tyrosinase positive albinism *(center column)*, and X-chromosomal ocular albinism *(right column)*. Foveal hypoplasia, reduced visual acuity, and VEP misrouting are common features regardless of mode of inheritance or phenotypic expression.